Journal of Materials Chemistry B

Accepted Manuscript

ROYAL SOCIETY OF CHEMISTRY

www.rsc.org/materialsB

Journal of Materials Chemistry B

ARTICLE

Multifunctional PEG-PLL Drug Conjugate Forming Redox-Responsive Nanoparticle for Intracellular Drug Delivery

Received 00th January 20xx,
Accepted 00th January 20xx

DOI: 10.1039/x0xx00000x

www.rsc.org/

Zhuxian Zhou,[a, b,*] Jianbin Tang,[a] Qihang Sun,[b] William J. Murdoch[c] and Youqing Shen[a,*]

Tumor-targeted, redox-responsive and high drug-loaded nanoparticles were synthesized from poly(ethylene glycol)-b-poly(L-lysine) (PEG-PLL) for enhanced cancer therapy. Hydrophobic drug camptothecin (CPT) was anchored to the lysine residual amines in PEG-PLL via disulfide bonds. Folate acid as targeting group was further introduced to the PLL block via long PEG chains. The conjugate self-assembled into nanoparticles of around 100 nm with hydrophobic CPT moieties forming the core and folate acid targeting groups on the shell. The nanoparticles were expected to be stable in the blood circulation but once internalized via folate receptor-mediated endocytosis, disintegrate and release the drug by glutathione in the cytosol. The nanoparticles could be as a nanocarrier to further encapsulate other drugs such as doxorubicin for combined chemotherapy. The CPT-conjugated nanoparticles had comparable cytotoxicity to free CPT at low doses but higher cytotoxicity than CPT at high doses.

1. Introduction

Polymers,[1, 2] dendrimers,[3-5] Polymer micelles,[6] liposomes,[7] and nanoparticles[8-10] have been extensively investigated as nanometer-sized carriers to deliver conventional anticancer drugs. These drug carriers can provide several distinct advantages for these drugs, such as improved solubility, enhanced stability by protecting it from degradation, prolonged circulation in blood compartments,[11-13] preferential accumulation in tumor tissue by passive targeting via the enhanced permeability and retention (EPR) effect of tumors[14] and by active targeting through tumor targets such as folate acid[15, 16] and EGF[17, 18].

The stability of drug delivery vehicles is critical for their intravenous drug retention and efficient tumor drug delivery.[5, 12, 19] Drugs are generally loaded in polymer micelles or nanoparticles via physical trapping by hydrophobic-hydrophobic interaction, but micelles or core-shell nanoparticles are at equilibrium with their unimers. Upon iv administration, dilution and nonspecific uptake of the unimers would dissociate the micelles, causing severe burst drug release before reaching tumor tissues.[20] One approach to overcome these problems is to conjugate drugs to the nanoparticles core via cleavable linkers triggered by intracellular stimuli such as pH,[21-23] glutathione[24, 25] or enzymes,[26-28] enabling cytosolic drug release. For instance, Kataoka et al. designed drug-conjugated micelles using poly(ethylene glycol)-poly(amino acid) block copolymers. The anticancer drugs including doxorubicin (DOX) or cisplatin were anchored to the polymers by a hydrazone linkage which allows the polymeric micelles to release drugs selectively at acidic pH (4-6).[29, 30] More recently, Nicolas et al synthesized polymer-gemcitabine conjugate amphiphiles by living radical polymerization. These drug-polymer conjugates self-assembled in aqueous solution to form stable, narrowly-dispersed nanoparticles and showed significant anticancer activity.[31]

Camptothecin (CPT), a plant alkaloid extracted from Camptotheca acuminate, has potent antitumor properties that derives from its inhibiting the nuclear enzyme topoisomerase I, but its clinical use has been severely hampered by its severe side effects and instability of its E-lactone ring.[32] Conjugating CPT via its C-20-OH to water-soluble polymers can stabilize the lactone ring, improve solubility, increase blood circulation time, and enhance tumor uptake, and thereby significantly improve CPT's efficacy. Thus, many novel nanocarriers such as polymers (PEG,[33, 34] HPMA,[35] cyclodextrin-containing polymers,[36] et al), liposomes,[37, 38] dendrimers,[39, 40] and nanoparticles[41] have been proposed as CPT delivery systems promising results either pre-clinically or clinically has been achieved.[42]

[a] Center for Bionanoengineering and State Key Laboratory for Chemical Engineering, Department of Chemical and Biological Engineering, Zhejiang University, Hangzhou 310027, China. Email: zhouzx@zju.edu.cn or shenyq@zju.edu.cn
[b] Department of Chemical and Petroleum Engineering, University of Wyoming, Laramie, WY 82071, United States.
[c] Department of Animal Science, University of Wyoming, Laramie, WY 82071, United States.

Herein, we report tumor-targeted CPT-conjugate nanoparticles, with redox-sensitive intracellular drug release for CPT delivery. CPT was conjugated to the amine groups of block-polylysine (PLL) via disulfide bonds. A tumor-targeting ligand folate acid was attached to the PLL amines via PEG chain. The amphiphilic CPT-conjugate formed stable nanoparticles with uniform sizes. These nanoparticles can be loaded with a secondary anticancer drug DOX (Scheme 1). The nanoparticles should disassociate once inside tumor cells with elevated glutathione (GSH) concentration (~ 10 mM[43]) via the cleavage of the disulfide linker and the CPT moieties. This approach has advantages including tunable drug loading and particular size, super stability in blood and rapid drug release in tumor, enhanced tumor uptake via both folate-targeted nanoparticles and EPR effect of the tumor.

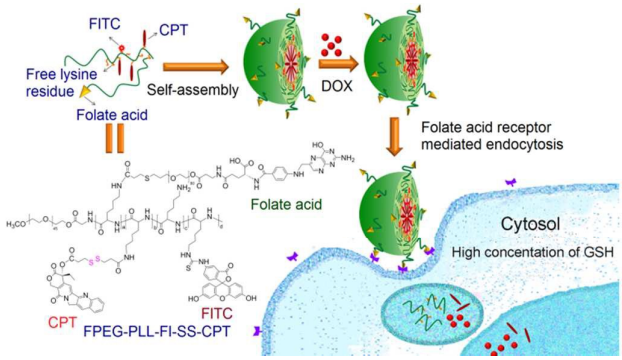

Scheme 1. FPEG-PLL self-assembles into CPT-cored nanoparticles and another anticancer drug DOX is loaded into the nanoparticles; these nanoparticles are stable in blood stream and internalized by FA-receptor mediated endocytosis; the nanoparticles disassociate once inside tumor cells with elevated GSH concentration (~ 10 mM) via the cleavage of the disulfide linker and the CPT moieties; the released DOX and CPT can enter the cell cytosol and nucleus for pharmaceutical actions.

2. Experimental

2.1. Materials. PEG methyl ether methacrylate (Mn = 2000), cysteamine, trifluoroacetic acid (TFA), hydrobromic acid (HBr), acetic acid (AcOH), fluorescein isothiocyanate isomer I (FITC), *N*-(*tert*-butoxycarbonyl)glycine (Boc-Gly-OH), cyclohexyl carbodiimide (DCC), *N*-hydroxysuccinimide (NHS) , *N,N*-diisopropylethylamine (DIPEA), *N*-(3-dimethylaminopropyl)-*N'*-ethylcarbodiimide hydrochloride (EDC), folate acid, (S)-(+)-camptothecin (CPT), and doxorubicin (DOX) were purchased from Sigma-Aldrich and used as received. α-Folic acid-ω-carboxylic acid functionalized PEG (Folate-PEG_{80}-COOH, Mn = 3500),[44] and ε-benzyloxycarbonyl-l-lysine *N*-carboxyanhydride ((NCA)-lysine-z)[45] were synthesized according to the literature.

2.2. Synthesis of the amphiphilic CPT-drug conjugates (Scheme. 2).

2.2.1. Preparation of PEG-block-poly(L-lysine) (PEG_{45}-PLL_{25}). (NCA)-Lysine-z (3 g, 9.8 mmol) was dissolved in dry DMF (10 ml) and degassed. PEG_{45}-NH_2 (0.84 g, 0.39 mmol) in dry THF (5 ml) was added to the solution. The mixture was stirred under N_2 at room temperature for 24 h and then at 40 °C for additional 48 h. The solution was concentrated and poured into ethyl ether (200 ml). The precipitate was washed with ethyl ether and dried under vacuum. The yield was 75%. No free PEG was observed by gel permeation chromatography (GPC) with DMF as eluent. The composition of PEG-PLL-z was determined by ^{1}H NMR. PEG-PLL-z (1 g) was dissolved in TFA followed by adding 4-fold of a 33 wt % solution of HBr in AcOH. The reaction mixture was stirred for 1 h at room temperature. The reaction mixture was then poured into ethyl ether. The precipitate PEG_{45}-PLL_{25}·HBr was collected and dried in vacuum. PEG_{45}-PLL_{25}·HBr was dissolved in water and the solution pH was adjusted to 9.0. The solution was then dialyzed (Spectra/Pro MWCO = 1000) against water (1 L × 3) and lyophilized to obtain PEG_{45}-PLL_{25}. The yield was 68%. PEG-PLL-z: ^{1}H NMR (400 MHz, DMSO-d_6, δ): 7.44-7.26 (br, ArH), 4.98 (br, ArCH_2), 4.2-3.9 (br, -NH-CH(CH_2-)(C=O)-), 3.51 (br, -OCH_2CH_2- of PEG), 2.90 (br, $CH_3(CH_2)_2CH_2$NH(C=O)-), 1.8-1.2 (br, $CH_3(CH_2)_2CH_2$NH(C=O)-). PEG-PLL (400 MHz, D_2O, δ): 4.18 (br, -NH-CH(CH_2-)(C=O)-), 3.56 (br, -OCH_2CH_2- of PEG), 2.88 (t,-CH_2NH_2), 1.64-1.56 (m, -$CH_2CH_2CH_2CH_2NH_2$), 1.32 (m, -$CH_2CH_2CH_2CH_2NH_2$).

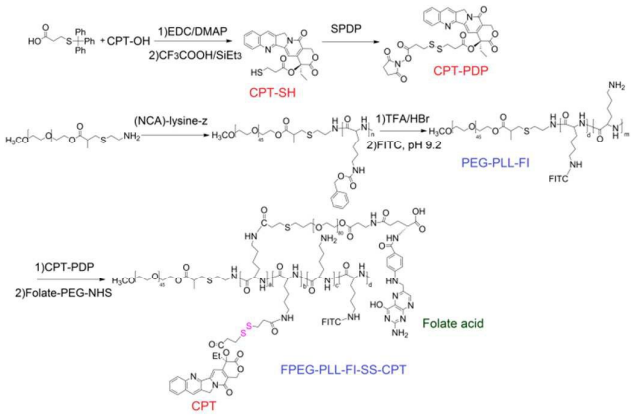

Scheme 2. Synthesis of the folic acid-functionalized FITC-labeled CPT-conjugates with PEG- block-PLL (FPEG-PLL-FI-SS-CPT).

2.2.2. Preparation of FITC labeled PEG-PLL (PEG_{45}-PLL_{25}-$FI_{1.5}$). PEG_{45}-PLL_{25} (200 mg, 0.038 mmol) was dissolved in water (6 ml) and the pH was adjusted to 9.4 using 1M NaOH. FITC (30 mg, 0.076 mmol) was added to this solution. The mixture was stirred overnight in dark and dialyzed (Spectra/Pro MWCO = 1000) against water (1 L × 4). The solution was lyophilized to give a yellowish solid with a yield of 85%. The FITC content was determined by UV spectrum at 495 nm (ε_{495}=75,800$M^{-1}cm^{-1}$).

2.2.3. Preparation of camptothecin-3-(2-pyridyldithio) propionyl (CPT-PDP).[13] CPT (348 mg, 1.0 mmol), 3-tritylsulfanylpropionic acid (348 mg, 1.0 mmol), DMAP (134 mg, 1.1 mmol) and EDC (210 mg, 1.1 mmol) were mixed in anhydrous dichloromethane (50 ml). The solution was stirred overnight at room temperature and then filtered and the solvent was removed by rotary evaporation. The residue was dissolved in anhydrous dichloromethane (14 ml), and a mixture solution of triethylsilane (2 ml) and trifluoroacetic acid

(TFA) (4 ml) was added. After stirring at room temperature for 2 h, dichloromethane and TFA were removed by evaporation. The crude product was redissolved in dichloromethane and the solution was poured in an excess of cold ethyl ether. The precipitate was isolated and dried in vacuum. A yellowish powder with a purity of 92% (according to ^{1}H NMR) was obtained with a yield of 80%. ^{1}H NMR (400 MHz, DMSO-d_6, δ) of CPT-SH: 8.62 (s, 1H), 8.07 (m, 2H), 7.80 (m, 1H), 7.65 (m, 1H), 7.11(s, 1H), 5.45 (s, 2H), 5.22 (s, 2H), 2.83 (t, 2H), 2.66 (m, 2H), 2.45 (m, 1H), 2.12 (m, 2H), 0.88 (t, 3H).

CPT-SH (1 g, 2.3 mmol) was dissolved in dichloromethane (30 ml) followed by adding SPDP (1.04 g, 3.4 mmol). The mixture was stirred at room temperature for 3 h, and some of CPT-PDP would precipitate out from the solution. Thin-layer chromatography (CH_3Cl : MeOH = 1 : 0.05) was used to confirm all CPT-SH was reacted. The mixture was then concentrated and poured into ethyl ether. The precipitate was isolated and dried in vacuum to obtain a light yellow solid. The yield was 93%. ^{1}H NMR (400 MHz, DMSO-d_6, δ) of CPT-PDP: 8.69 (s, 1H), 8.14 (d, 1H), 7.85 (d, 1H), 7.71 (m, 1H), 7.17 (s, 1H), 5.50 (s, 2H), 5.29 (s, 2H), 3.08-2.93 (m, 8H), 2.78(s, 4H) and 2.15 (m, 2H), 0.92 (t, 3H).

2.2.4. Preparation of PEG_{45}-PLL_{25}-SS-$CPT_{3,\ 6\ or\ 8}$ and PEG_{45}-PLL_{25}-$FI_{1.5}$-SS-CPT_6. PEG_{45}-PLL_{25} (50 mg, 0.0096 mmol) was dissolved in DMSO (3 ml) and degassed. DIPEA(10 μl) was added to the solution. CPT-PDP (18.3 mg, 0.029 mmol) in DMSO (2 ml) was then added to the solution under N_2. The mixture was stirred under N_2 at room temperature for 4 h. The reaction was tracked by HPLC. The mixture was then dialyzed (Spectra/Pro MWCO=1000) against acetonitrile (100 ml). The precipitate was collected, washed with acetonitrile three times and dried in vacuum to obtain PEG_{45}-PLL_{25}-SS-CPT_3. The yield was 65%. PEG_{45}-PLL_{25}-SS-$CPT_{6\ or\ 8}$ and PEG_{45}-PLL_{25}-$FI_{1.5}$-SS-CPT_6 were prepared similarly by adding corresponding amounts of CPT-PDP. The products were characterized by ^{1}H NMR, UV-Vis spectra and HPLC.

2.2.5. Preparation of folic acid-functionalized conjugate, FPEG-PLL-FI-SS-CPT. Folate-PEG_{80}-COOH was mixed with EDC and NHS (molar ratio 1:2:2). The solution was stirred for 1 h and added to the reaction solution of PEG-PLL-FI and CPT-PDP under N_2. The mixture was kept stirring for 3 h and then dialyzed (Spectra/Pro MWCO=1000) against acetonitrile followed by dialyzing (Spectra/Pro MWCO=3000) against water. FPEG-PLL-FI-SS-CPT was obtained by lyophilization.

2.3. Preparation of control CPT-drug conjugates (PEG-PLL-CPT without disulfide bond) (Supporting scheme 1)

2.3.1. Preparation of camptothecin succinate (CPT-COOH)

CPT (500 mg, 1.44 mmol), mono-t-butyl succinate (500 mg, 2.86 mmol), DMAP (350 mg, 2.86 mmol) and EDC (545 mg, 2.86 mmol) were mixed in anhydrous dichloromethane (70 ml). The solution was stirred overnight at room temperature and the cloudy solution was turned to clear. Solvent was then removed by rotary evaporation. The residue was dissolved in trifluoroacetic acid (15 ml) and stirred at room temperature for 4 h. TFA was removed by rotary evaporation. The crude product was dissolved in DMSO (3 ml) and ethanol (30 ml) was added to the solution. The precipitate was isolated, washed with ethanol and dried in vacuum. A yellowish powder was obtained with a yield of 85%. ^{1}H NMR (400 MHz, DMSO-d_6, δ) of CPT-COOH: 12.25 (br, 1H), 8.70 (d, 1H), 8.18 (m, 2H), 7.87 (m, 1H), 7.73 (m, 1H), 7.14 (s, 1H), 5.49 (s, 2H), 5.31 (s, 2H), 2.77 (m, 2H), 2.46 (m, 2H), 2.14 (m, 2H), 0.91 (t, 3H).

2.3.2. Preparation of PEG_{45}-PLL_{25}-CPT_6 (without disulfide bond).

PEG_{45}-PLL_{25} (50 mg, 0.0096 mmol) was dissolved in DMSO (3 ml) and DIPEA (10 μl) was added to the solution. CPT-COOH (25.8 mg, 0.058 mmol) in DMSO (2 ml) and EDC (13.2 mg, 0.070 mmol) were then added to the previous solution. The mixture was stirred at room temperature for 4 h. The solution was then dialyzed (Spectra/Pro MWCO=1000) against acetonitrile (100 ml). The precipitate was collected, washed with acetonitrile three times. The crude product was then dissolved in DMSO and dialyzed (Spectra/Pro MWCO=1000) against water (500 ml × 3). The product was obtained by lyophilization with a yield of 58%.

2.4. Fabrication of the CPT-conjugated nanoparticles and DOX-loading. 2 mg of PEG_{45}-PLL_{25}-SS-CPT_x (x = 3, 6 or 8) or PEG_{45}-PLL_{25}-CPT_6 (control drug conjugate, without disulfide bond) was dissolved in 1 ml DMF and filtered (0.45 μm). The solution was then dialyzed (Spectra/Por, MWCO=3500) against water (48 h, 1L×4). The nanoparticles could also be made by directly dispersing the conjugate in water with ultrasound. To load DOX into the nanoparticles, DOX base (0.5 mg) was dissolved with the conjugate in DMF (1 mg/ml, 1 ml) and stirred for 1 h. The mixture was then dialyzed (Spectra/Por, MWCO=3500) against water (24 h, 1L×4). DOX loading content was analyzed by HPLC. Nanoparticles made from PEG_{45}-PLL_{25}-FI-SS-CPT_x or $FPEG_{45}$-PLL_{25}-FI-SS-CPT_x were fabricated similarly.

2.5. Reverse-phase HPLC. Ion-pairing reverse-phase HPLC (RP-HPLC) was performed on a RP-C18 HPLC column (250 × 4.6 mm^2, 5 micrometers). Isocratic and gradient elution was used to study the drug release and characterize the products. Eluant A was water containing 0.1% TFA and B was acetonitrile containing 0.1% TFA. The mobile phase for isocratic elution was run with 50% A and 50% B at a flow rate of 1.3 ml/min for 30 min. The volume of each injection was 100 μl, and the detection of eluted samples was performed at 360 nm.

2.6. Dynamic light scattering. The sizes (diameters) of nanoparticles were determined using a Nano-ZS zetasizer (Malvern Instrument Ltd., UK) with a laser light wavelength of 632.8 nm at a scattering angle at 173°. The zetasizer was routinely calibrated with a 60 nm nanosphere™ standard (Duke Scientific Corp. CA). Each measurement was performed in triplicate, and the results were processed with DTS software version 3.32.

2.7. Observation of the nanoparticles using transmission electron microscopy (TEM) or confocal laser scanning fluorescence microscopy. The nanoparticle solution (1 mg/ml, 10 μl) was applied onto a 150-mesh carbon-coated copper

grid. The excess solution was wiped off with filter paper. A droplet of 2% (w/v) aqueous uranyl acetate solution was then deposited onto the dried samples. The excess solution of the staining agent was removed with a piece of filter paper. Images were recorded using a transmission electron microscope (HITACHI H-7000 TEM) operated at a voltage of 75 kV.

The FITC labeled CPT-conjugated nanoparticles were prepared as described above. The nanoparticle solution (1 mg/ml) (3 µl) was dropped on a glass slide and covered with a cover glass. The images were taken with a Leica TCS SP2 confocal microscope. FITC was excited using a 488-nm laser and the emission wavelength was read from 505 to 530 nm and expressed as green. Images were processed with NIH ImageJ and the original magnification was 63×.

2.8. Critical micelle concentration (CMC) determination. The CMC values of the polymers were determined using the method we reported previously.[13]

2.9. Drug release study. 4 ml of DOX-loaded nanoparticles (1 mg/ml) in PBS (pH 7.4, 10 mM) were loaded into two dialysis tubing (MWCO 3500 Da). The dialysis tubing was immersed in 100 ml of pH 7.4 PBS buffer at 37°C with gentle shaking. For DTT-triggered CPT release experiment, DTT (10 mM) was added to the buffer solution. At timed intervals, 50 µL of the solution in the tubing was sampled for analyzing CPT release and 0.5 ml of the solution in the buffer was sampled for analyzing DOX release. The solution in the tubing was homogenized before sampling. The CPT release was analyzed by HPLC with UV detector. The UV spectra of PEG_{45}-PLL_{25}-SS-CPT_x at different time point were obtained from HPLC after its separation from free CPT. The DOX released was studied by measuring its UV absorbance at 480 nm (ε_{480} = 11500 $M^{-1}cm^{-1}$) using a micro UV cuvette.

2.10. Cell culture. SKOV-3 and OVCAR-3 ovarian cancer cells, MDA-MB-468 and MCF-7 breast cancer cells were purchased from American Type Culture Collection (ATCC, Manassas, VA). Cells were cultured in RPMI-1640 medium containing 10% fetal bovine serum (FBS), 10 µg/ml insulin, and 1% antibiotic/antimycotic solution (Sigma A9909) at 37 ^{o}C in a 5% CO_2 environment. The cells used for cellular uptake and in vitro cytotoxicity assay of the FA-functionalized nanoparticles were cultured in folic-free medium ((Invitrogen Corp., Carlsbad, CA) for at least two weeks before use.

2.11. Cellular uptake and intracellular localization of the nanoparticles observed using confocal fluorescence microscopy. For folate receptor-mediated cellular uptake study, cells were incubated with FITC-labeled FPEG-PLL-FI-SS-CPT or PEG-PLL-FI-SS-CPT nanoparticles (7 µM polymer, according to FITC) at 37 ^{o}C and 5% CO_2 for 4 h. For the intracellular colocalization study, cells were incubated with FPEG-PLL-FI-SS-CPT nanoparticles for 4 h first. LysoTracker Red DND-99 (Molecular Probes, Eugene, OR) (150 × 10^{-3} µM) was then added and the cells were incubated for another 2 h. The cells were then thoroughly washed with PBS at 4 ^{o}C three times and observed using confocal microscopy for the colocalization of the nanoparticles and lysosomes. For observation of nuclear localization of the nanoparticles, the cells were incubated with DOX-loaded nanoparticles (7 µM, containing DOX 4 µg/ml) at 37 ^{o}C and 5% CO_2 for 12 h. DRAQ 5 nuclei dye (1 µl) (Biostatus, 5 × 10^{-3} M) was added just before the observation. Images were obtained using a Leica TCS SP2 microscope. FITC was observed using Ar/ArKr 458/488 nm laser and the emission wavelength was read from 505 to 530 nm and expressed as green. DOX was observed using Ar/ArKr 458/488 nm laser and the emission wavelength was read from 560 to 610 nm and expressed as red. LysoTracker was observed using a GreNe 543 nm laser and the emission wavelength was read from 523 to 563 nm and expressed as red. DRAQ 5 nuclei dye was observed using a HeNe 633 nm laser and the emission wavelength was read from 660 to 760 nm and expressed as blue. Images were produced by using the lasers sequentially with a 63 × objective lens. Cells were kept at 37 °C and 5% CO_2 except when being observed on the microscope. Images were processed with NIH ImageJ.

2.12. In vitro cytotoxicity assay. The cytotoxicity assay was carried out using the MTT cell proliferation assay kit (ATCC, Manassas, VA) according to the modified manufacturer's protocol. Cells were cultured in folic-free medium (Invitrogen Corp., Carlsbad, CA) for at least two weeks before use. They were then seeded onto 96-well plates and incubated for 24 h. The original medium (200 µl) was removed and replaced with the nanoparticles or free CPT solutions at different doses and incubated for 24 h. The medium in each well was then replaced with fresh cell culture medium and further incubated for 24 h. MTT reagent (10 µl) was then added to each well and incubated for 6 h until purple precipitates were visible. Finally, the detergent reagent (100 µl) was added to each well, and the plates were incubated at 37 ^{o}C for 18 h or until all the crystals dissolved. The absorbance intensity at 570 nm was recorded and the cytotoxicity was expressed as a percentage of the control.

3. Results and Discussion

3.1. Design and Synthesis of Amphiphilic GSH-sensitive CPT Nanoparticles

The synthesis of FPEG-PLL-FI-SS-CPT_x is shown in Scheme. 2 and its structure was confirmed by ^{1}H NMR (Fig. 1), UV-vis spectrum (Fig. 2) and HPLC (Fig. 3). PEG_{45}-PLL_{25} was synthesized by PEG_{45}-NH_2 (Mn = 2000) initiated ring-opening polymerization of (NCA)-lysine-z, followed by deprotection of *tert*-butoxycarbonyl groups with TFA. The repeating units of lysine groups in the block polymer was controlled by the molar feed ratio of the monomer (NCA)-lysine-z to PEG_{45}-NH_2, and the value was confirmed by ^{1}H NMR spectra. A fluorescent dye, FITC, was introduced to the PLL block and its content was determined by UV-Vis spectra (ε_{495} = 75,800 $M^{-1}cm^{-1}$) to be 1.5 FITC molecules per chain. CPT-PDP was synthesized by the reaction of CPT-SH and a heterobifunctional coupling reagent SPDP,[13] characterized by ^{1}H NMR spectrum and the HPLC. The CPT content in the copolymer was controlled by the molar

feed ratio of CPT-PDP to PEG_{45}-PLL_{25}. Unreacted CPT-PDP (< 5%) was removed by extracting with acetonitrile. Adding CPT-PDP at molar ratio of 3, 6 or 8 relative to PEG_{45}-PLL_{25} chain produced PEG_{45}-PLL_{25}-SS-CPT_x with x of 2.95, 6.1 and 8.05, respectively, as calculated from the integration intensities of the -CH_3 in CPT and the -CH_2- in lysine in their ^{1}H NMR spectra (Fig. 1B). These data were in agreement with the results from the HPLC analysis according to the standard CPT curve (2.90, 5.92 and 7.93, respectively).

PEG_{45}-PLL_{25}-SS-CPT_6 was selected for further functionalization with folic acid via PEG chain (3500 Da) by the reaction of the lysine residue amines with NHS-activated PEG-FA. The molar ratio of FA to the PEG_{45}-PLL_{25}-SS-CPT_6 chain was kept at 10:1. The resulting folic acid functionalized conjugate

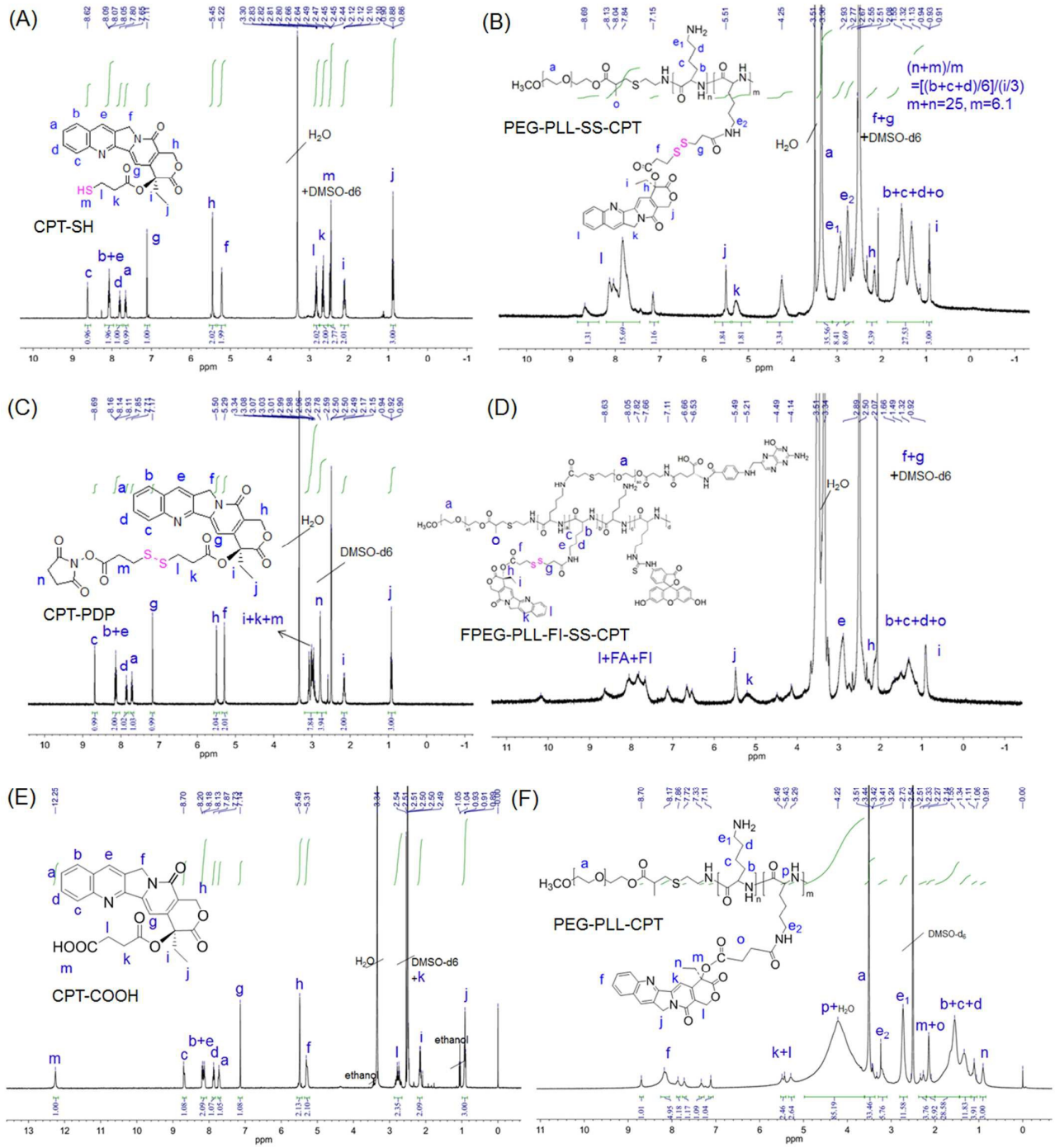

Fig. 1 The ^{1}H NMR spectra of CPT-SH (A), PEG_{45}-PLL_{25}-SS-CPT_6 (B), CPT-PDP (C), $FPEG_{45}$-PLL_{25}-$FI_{1.5}$-SS-CPT_6 (D), CPT-COOH (E) and PEG_{45}-PLL_{25}-CPT_6 (F)) in DMSO-d_6.

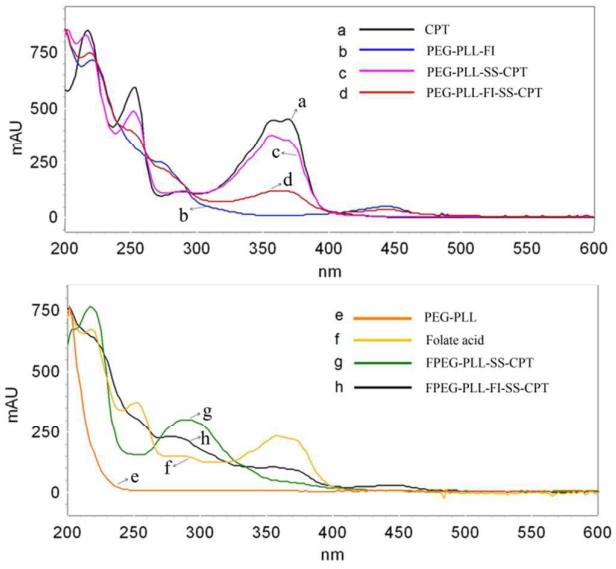

Fig. 2 The UV-vis spectra of CPT (a), PEG_{45}-PLL_{25}-FI (b), PEG_{45}-PLL_{25}-SS-CPT_6 (c), PEG_{45}-PLL_{25}-FI-SS-CPT (d), PEG_{45}-PLL_{25} (e), Folic acid (f), $FPEG_{45}$-PLL_{25}-SS-CPT_6 (g) and $FPEG_{45}$-PLL_{25}-FI-SS-CPT_6 (h) in water.

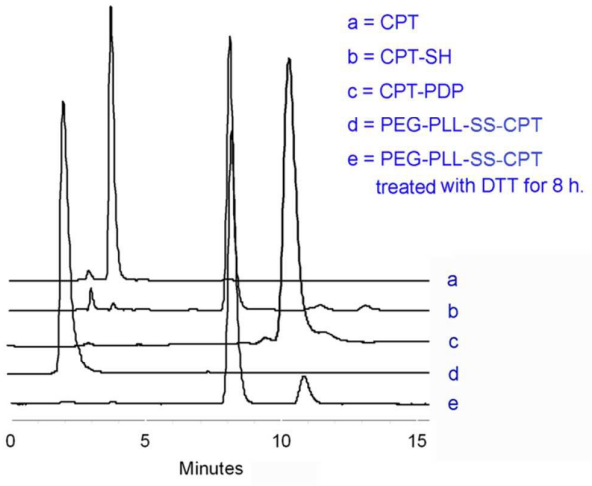

Fig. 3 The HPLC traces of CPT (a), CPT-SH (b), CPT-PDP (c), PEG_{45}-PLL_{25}-SS-CPT_6 (d) and PEG_{45}-PLL_{25}-SS-CPT_6 treated with DTT for 8 h (e). HPLC method: isocratic elution with 50% ACN.

($FPEG_{45}$-PLL_{25}-SS-CPT_6) was characterized by ^{1}H NMR and UV (Fig. 2) spectra. The typical UV-vis absorbance of FA in $FPEG_{45}$-PLL_{25}-SS-CPT_6 indicates the conjugation of FA to PEG_{45}-PLL_{25}-SS-CPT_6.

PEG_{45}-PLL_{25}-SS-CPT_x formed nanoparticles in aqueous solution due to the hydrophobicity of CPT. The CMCs of PEG_{45}-PLL_{25}-SS-$CPT_{3,\ 6\ or\ 8}$ were measured using nile red[13] to be 0.094, 0.066 and 0.054 mg/ml, respectively (Fig. 4A). The micelle morphologies of PEG_{45}-PLL_{25}-SS-$CPT_{3,\ 6\ or\ 8}$ were observed using TEM (Fig. 5A-C) and confocal fluorescence microscopy (Fig. 5F). The size observed by confocal fluorescence microscopy was larger than its actual size due to limitation of resolution in confocal microscopy. They all were spherical and the sizes increased as the CPT content increased. The sizes and size distribution of the nanoparticles were further quantitated by DLS (Fig. 4B). The diameter of PEG_{45}-PLL_{25}-SS-$CPT_{3,\ 6\ or\ 8}$ were 85, 118, and 152 nm, respectively. The PEG_{45}-PLL_{25}-SS-CPT_6 nanoparticles could be loaded with 10.2 wt% of DOX at an efficiency of 65%. Loading DOX to PEG_{45}-PLL_{25}-SS-CPT_6 increased the sizes of the nanoparticles (Fig. 5E). A control CPT-nanoparticle (PEG_{45}-PLL_{25}-CPT_6) without GSH-sensitivity was prepared and characterized for comparison (Supporting scheme 1, Fig. 1 E and F, and Supporting Fig. 1).

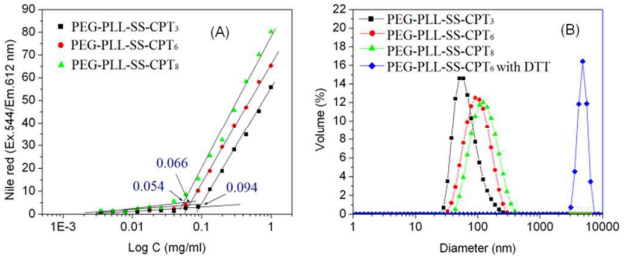

Fig. 4 (A) Determination of the CMCs: the fluorescence intensity of nile red as a function of the PEG-PLL-CPT concentration. (B) Micelle sizes measured by dynamic light scattering of PEG_{45}-PLL_{25}-SS-CPT_x, and PEG_{45}-PLL_{25}-SS-CPT_6 after treated with 10 mM DTT for 8 h.

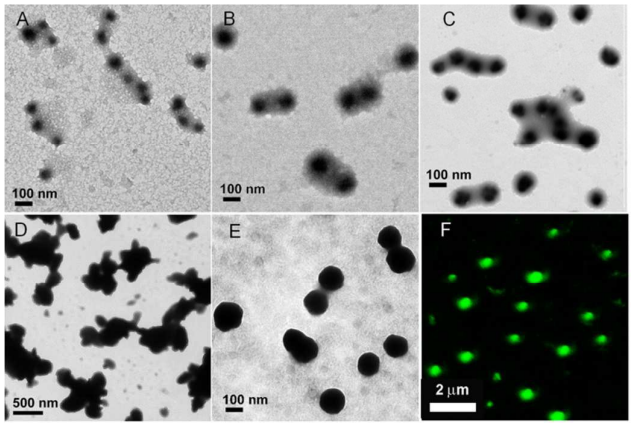

Fig. 5 The TEM images of the nanoparticles of PEG_{45}-PLL_{25}-SS-CPT_3 (A), PEG_{45}-PLL_{25}-SS-CPT_6 (B), PEG_{45}-PLL_{25}-SS-CPT_8 (C), PEG_{45}-PLL_{25}-SS-CPT_6 after treated with DTT for 8 h (D), PEG_{45}-PLL_{25}-SS-CPT_6 loaded with DOX (E). The confocal florescence images of PEG_{45}-PLL_{25}-$FI_{1.5}$-SS-CPT_6 observed from the FITC channel (F). The conjugate concentration is 1 mg/ml.

3.2 Redox-Responsive Drug Release and Micelle Collapse

These nanoparticles were stable in PBS over one week. No CPT was released from the nanoparticles and the nanoparticles did not change in size or size distribution. Once treated with 10 mM GSH or DTT (a strong reducing agent similar with GSH), CPT was released and precipitated out from the solution. The typical UV absorption of CPT moieties in PEG_{45}-PLL_{25}-SS-CPT_x decreased with the release of CPT as determined by HPLC separation followed with UV examination (Fig. 6A). Up to 92% of CPT was released from the nanoparticles within 8 h (Fig. 6B). Correspondingly, the nanoparticles collapsed as observed by TEM (Fig. 5D) and DLS (Fig. 6B). The size changes of PEG_{45}-PLL_{25}-SS-CPT_6 after treated with GSH (10 mM) at different time interval were studied by DLS (Supporting Fig.2). DOX release was also accelerated from the DOX-loaded CPT-cored nanoparticles. The DOX release was 36% in 24 h in the absence of DTT while the value was 68% in the present of DTT (10 mM) (Fig. 6B). At the same condition, no similar phenomena were found with the control nanoparticle (PEG_{45}-PLL_{25}-CPT_6). These results suggest that the GSH-sensitive CPT-conjugate nanoparticles would be stable in the blood stream and no CPT would be released in the blood. As soon as they reach the intracellular environment of tumor cells, in the abundant GSH would cleave the disulfide bonds in CPT-linker, resulting in fast release of CPT and entrapped DOX.

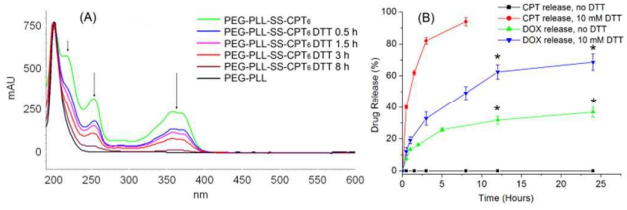

Fig. 6 CPT-release study: The UV-VIS spectra of PEG_{45}-PLL_{25}-SS-CPT_6 cultured with 10 mM DTT in PBS (pH 7.4, 50 mM), normalized with the point at 210 nm (A), and the corresponding time dependent CPT and DOX release with or without DTT (B). (*) $P < 0.01$.

3.3 Folate Receptor-Mediated Endocytosis and Subcellular Distribution

The folate receptor-mediated endocytosis and intracellular trafficking of $FPEG_{45}$-PLL_{25}-$FI_{1.5}$-SS-CPT_6 nanoparticles was observed with confocal laser light fluorescence. The FA-targeting $FPEG_{45}$-PLL_{25}-$FI_{1.5}$-SS-CPT_6 or FA-free PEG_{45}-PLL_{25}-$FI_{1.5}$-SS-CPT_6 nanoparticles were cultured with the cells for 4 h. With the FA groups, $FPEG_{45}$-PLL_{25}-$FI_{1.5}$-SS-CPT_6 can easily enter the cells and showed relatively high fluorescent intensity (Fig.7 A). In contrast, few PEG_{45}-PLL_{25}-$FI_{1.5}$-SS-CPT_6 was observed inside the cells (Fig. 7 B and C). The enhanced cellular uptake of $FPEG_{45}$-PLL_{25}-$FI_{1.5}$-SS-CPT_6 demonstrated the active targeting function of folate acid groups via folate receptor-mediated endocytosis. A subcellular compartment labeling method was used to observe the subcellular distribution of $FPEG_{45}$-PLL_{25}-$FI_{1.5}$-SS-CPT_6 nanoparticles in SKOV-3 cells (Fig. 7 D-F). The fluorescence of FITC in CPT-nanoparticles was expressed as green. LysoTracker was used to label late endosomes/lysosomes and displayed as red. The overlay of the two fluorescence images showed yellow spots, which indicates that nanoparticles were localized in endosomes/lysosomes after culturing with cells for 6 h.

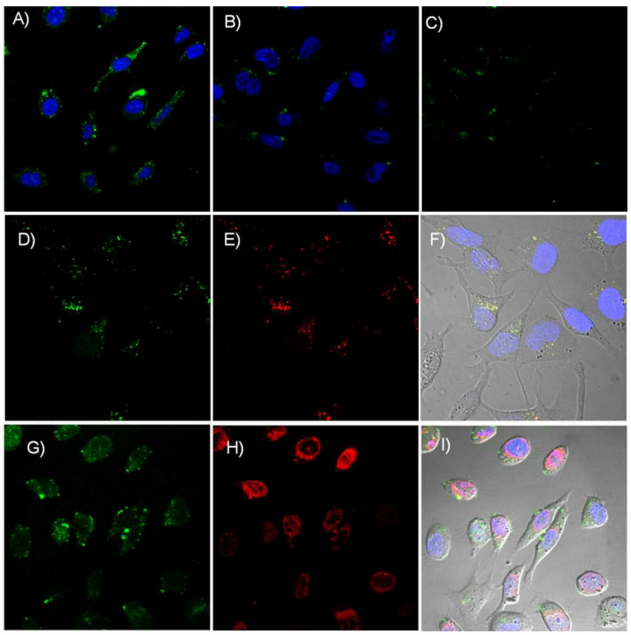

Fig. 7 Cellular uptake and subcellular localization of the nanoparticles observed by confocal laser scanning fluorescence microscopy. (A-C) Observation of folate-targeting groups enhanced cellular uptake: SKOV-3 cells were incubated for 2 h with folate acid functionalized CPT-nanoparticles ($FPEG_{45}$-PLL_{25}-$FI_{1.5}$-SS-CPT_6) (A, FITC overlay with nuclear dye) or FITC-labeled nanoparticles (PEG_{45}-PLL_{25}-$FI_{1.5}$-SS-CPT_6) (B, FITC overlay with nuclear dye; C, FITC channel) at a dose of 7 μM-equivalent to FITC; nuclear dye was added before observation. (D-F) Observation of the lysosomal localization: SKOV-3 cells were incubated with $FPEG_{45}$-PLL_{25}-$FI_{1.5}$-SS-CPT_6 (7 μM-equivalent to FITC) for 4 h and then cultured with LysoTracker (150 nM) for another 2 h; nuclear dye was added before observation. D) FITC channel, E) LysoTracker channel, F) overlay of D) and E) with nuclear dye and transmittance channel. Observation of DOX release in nucleus: SKOV-3 cells were incubated with $FPEG_{45}$-PLL_{25}-$FI_{1.5}$-SS-CPT_6/DOX (7 μM-equivalent to FITC, containing DOX 4 μg/ml) for 12 h; nuclear dye was added before observation. G) FITC channel, H) DOX channel, I) overlay of (G) and (H) with nuclear dye and transmittance channel.

Furthermore, as shown in Fig. 7 G-I, there were no green spots in the nuclei, indicating that the CPT-nanoparticles or the conjugates could not enter into the nucleus; they might be trapped in the endosomes/lysosomes. However, some DOX loaded in the nanoparticles localized in or associated with the nuclei, suggesting that DOX loaded in the CPT-nanoparticles could be burst released at an elevated concentration of GSH inside the cells where the disulfide bonds was broken and the CPT-nanoparticles was dissociated. It is believed that cell endosomes/lysosomes also have a high concentration of GSH but it is lower than cytosol which is the principle site of GSH biosynthesis. The released DOX was protonized and escaped from endosomes/lysosomes, entered into cytosol and finally diffused into the nuclei.

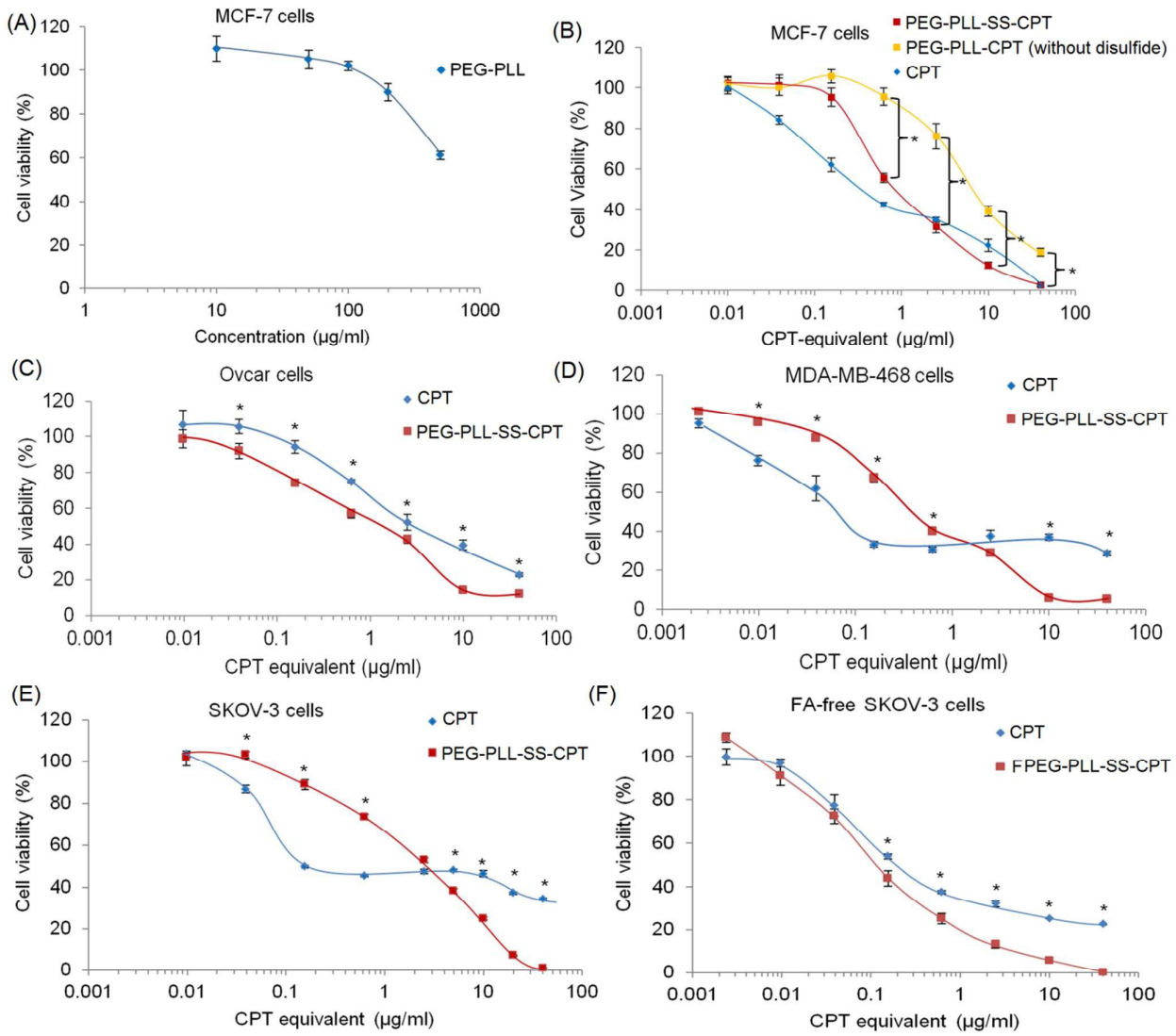

Fig. 8 The dose-responsive cytotoxicity of PEG_{45}-PLL_{25} (A) and PEG_{45}-PLL_{25}-CPT_6 (B) to MCF-7 cells, PEG_{45}-PLL_{25}-SS-CPT_6, $FPEG_{45}$-PLL_{25}-SS-CPT_6 and CPT to MCF-7 (B), OVCAR-3 (C), MDA-MB-468 (D) and SKOV-3 cells (E) as well as SKOV-3 cancer cells cultured in FA-free medium (F) with 24h treatment and 24 h post-treatment. Data represent mean ± s.d., n = 5. (*) $P < 0.01$.

3.4. In vitro cytotoxicity

The cytotoxicity of PEG_{45}-PLL_{25}, free CPT, PEG_{45}-PLL_{25}-CPT_6, PEG_{45}-PLL_{25}-SS-CPT_6 and $FPEG_{45}$-PLL_{25}-SS-CPT_6 to MCF-7, MDA-MB-468 breast cancer cells and SKOV-3, OVCAR-3 ovarian cancer cells were evaluated using the MTT assay. They were cultured with cells for 24 h, and then the cells were post-cultured for 48 h to allow the damaged cells to undergo apoptosis. The results are presented in Fig. 8. PEG_{45}-PLL_{25} showed low cytotoxicity to MCF-7 cells with IC_{50} higher than 500 μg/ml and it was expected to also have low cytotoxicity to other cell lines (Fig. 8A). PEG_{45}-PLL_{25}-SS-CPT_6 (IC_{50} = 0.88 μg/ml) showed much higher cytotoxicity than that of PEG_{45}-PLL_{25}-CPT_6 (IC_{50} = 6.8 μg/ml) to MCF-7 cells. The enhanced cytotoxicity of PEG_{45}-PLL_{25}-SS-CPT_6 indicated that the GSH-sensitive bond played an important role on inducing intracellular releasing of CPT (Fig. 8B). The IC_{50} values of free CPT to MCF-7, OVCAR-3, MDA-MB-468 and SKOV-3 cells were 0.34, 2.8, 0.061 and 0.17 μg/ml, respectively (Fig. 8B-F). The CPT-equiv. IC_{50} values of PEG_{45}-PLL_{25}-SS-CPT_6 to these cancer cells were 0.88, 1.9, 0.39 and 3.0 μg/ml. MDA-MB-468 cells were mostly sensitive and OVCAR-3 cells were mostly resistant to CPT. Comparing with free CPT, CPT-conjugate nanoparticle had higher cytotoxicity to OVCAR-3 cells and lower cytotoxicity to MCF-7, SKOV-3, MDA-MB-468 cells. The SKOV-3 cells showed resistance to free CPT at high doses due to its the low solubility but CPT in PEG_{45}-PLL_{25}-SS-CPT_6 had a good dose-responsive trend. CPT-nanoparticles showed comparable cytotoxicity with free CPT. The CPT-cored nanostructure can be dissociated by the diffusion of water-soluble GSH into the tight packed hydrophobic core and CPT moieties were released from the nanoparticles. However, the released CPT were in the form of CPT-thioester which need to be further hydrolyzed to parent CPT to exert their pharmaceutical effects.[13, 46] The FA-

functionalized nanoparticles had a higher cytotoxicity compared with non-FA-functionalized-nanoparticles. Its IC_{50} was as low as 0.13 μg/ml (free CPT, 0.20 μg/ml). This indicates that FA-targeting groups enhanced the cellular uptake of the nanoparticles, and once inside cells, the nanoparticles could effectively release CPT.

4. Conclusions

Tumor-targeting CPT-conjugated nanoparticles of high stability and cell-specific drug release were developed for cancer-targeted drug delivery. PEG-PLL was conjugated with a high content of CPT of via a disulfide bond and folic acid via PEG spacer. The conjugate formed CPT-cored nanoparticles with defined drug contents as high as 37.8%, while the nanoparticular size was tailorable by the CPT-content. Such nanoparticles enabled CPT and the loaded drug to be specifically released in cancer cell by GSH-triggered CPT-cleavage and nanoparticle collapse.

Acknowledgements

The authors thank the Major Program of National Natural Science Foundation of China (21090352), the National Natural Science Foundation (20974096, 21104065), the National Fund for Distinguished Young Scholars (50888001).

References

1. J. Kopecek, *Adv. Drug Deliv. Rev.*, 2013, **65**, 49-59.
2. M. E. Fox, F. C. Szoka and J. M. J. Fréchet, *Acc. Chem. Res.*, 2009, **42**, 1141-1151.
3. Z. Zhou and Z. R. Lu, *Nanomedicine-Uk*, 2014, **9**, 2387-2401.
4. Z. Zhou, X. Ma, C. J. Murphy, E. Jin, Q. Sun, Y. Shen, E. A. Van Kirk and W. J. Murdoch, *Angew. Chem. Int. Ed.*, 2014, **53**, 10949-10955.
5. Q. Sun, X. Sun, X. Ma, Z. Zhou, E. Jin, B. Zhang, Y. Shen, E. A. Van Kirk, W. J. Murdoch, J. R. Lott, T. P. Lodge, M. Radosz and Y. Zhao, *Adv. Mater.*, 2014, **26**, 7615-7621.
6. G. Y. Liu, C. J. Chen and J. Ji, *Soft Matter*, 2012, **8**, 8811-8821.
7. H. M. Kieler-Ferguson, J. M. J. Fréchet and F. C. Szoka Jr, *Wires Nanomed. Nanobi.*, 2013, **5**, 130-138.
8. J. Nicolas, S. Mura, D. Brambilla, N. Mackiewicz and P. Couvreur, *Chem. Soc. Rev.*, 2013, **42**, 1147-1235.
9. Z. Zhou, Y. Shen, J. Tang, E. Jin, X. Ma, Q. Sun, B. Zhang, E. A. Van Kirk and W. J. Murdoch, *J. Mater. Chem.*, 2011, **21**, 19114-19123.
10. P. Gou, W. Liu, W. Mao, J. Tang, Y. Shen and M. Sui, *J Mater Chem B*, 2013, **1**, 284-292.
11. A. Zhang, Z. Zhang, F. Shi, J. Ding, C. Xiao, X. Zhuang, C. He, L. Chen and X. Chen, *Soft Matter*, 2013, **9**, 2224-2233.
12. Q. Sun, M. Radosz and Y. Shen, *J. Control. Release*, 2012, **164**, 156-169.
13. Z. Zhou, X. Ma, E. Jin, J. Tang, M. Sui, Y. Shen, E. A. Van Kirk, W. J. Murdoch and M. Radosz, *Biomaterials*, 2013, **34**, 5722-5735.
14. H. Maeda, H. Nakamura and J. Fang, *Adv. Drug Deliv. Rev.*, 2013, **65**, 71-79.
15. Z. Zhou, Y. Shen, J. Tang, M. Fan, E. A. Van Kirk, W. J. Murdoch and M. Radosz, *Adv. Funct. Mater.*, 2009, **19**, 3580-3589.
16. W. Scarano, H. T. T. Duong, H. Lu, P. L. De Souza and M. H. Stenzel, *Biomacromolecules*, 2013, **14**, 962-975.
17. A. M. Master and A. Sen Gupta, *Nanomedicine-Uk*, 2012, **7**, 1895-1906.
18. Y. F. Wang, P. F. Liu, L. H. Qiu, Y. Sun, M. J. Zhu, L. Y. Gu, W. Di and Y. R. Duan, *Biomaterials*, 2013, **34**, 4068-4077.
19. C. Gao, Y. Wang, W. P. Zhu and Z. Q. Shen, *Chinese J. Polym. Sci.*, 2014, **32**, 1431-1441.
20. R. Tong and J. Cheng, *Macromolecules*, 2012, **45**, 2225-2232.
21. E. Jin, B. Zhang, X. Sun, Z. Zhou, X. Ma, Q. Sun, J. Tang, Y. Shen, E. Van Kirk, W. J. Murdoch and M. Radosz, *J. Am. Chem. Soc.*, 2013, **135**, 933-940.
22. C. L. Du, D. W. Deng, L. L. Shan, S. N. Wan, J. Cao, J. M. Tian, S. Achilefu and Y. Q. Gu, *Biomaterials*, 2013, **34**, 3087-3097.
23. L. Zhou, R. Cheng, H. Q. Tao, S. B. Ma, W. W. Guo, F. H. Meng, H. Y. Liu, Z. Liu and Z. Y. Zhong, *Biomacromolecules*, 2011, **12**, 1460-1467.
24. L. Y. Tang, J. Wang, Y. C. Wang, Y. Li and J. Z. Du, *Bioconjugate Chem.*, 2009, **20**, 1095-1099.
25. W. Zhu, Y. Wang, X. Cai, G. Zha, Q. Luo, R. Sun, X. Li and Z. Shen, *J Mater Chem B*, 2015, **3**, 3024-3031.
26. T. L. Andresen, D. H. Thompson and T. Kaasgaard, *Mol. Membr. Biol.*, 2010, **27**, 353-363.
27. S. H. Medina, M. V. Chevliakov, G. Tiruchinapally, Y. Y. Durmaz, S. P. Kuruvilla and M. E. H. ElSayed, *Biomaterials*, 2013, **34**, 4655-4666.
28. L. Jiang, Z. M. Gao, L. Ye, A. Y. Zhang and Z. G. Feng, *Polymer*, 2013, **54**, 5188-5198.
29. Y. Bae and K. Kataoka, *Adv. Drug Deliv. Rev.*, 2009, **61**, 768-784.
30. Y. Bae, S. Fukushima, A. Harada and K. Kataoka, *Angew. Chem. Int. Ed.*, 2003, **42**, 4640-4643.
31. S. Harrisson, J. Nicolas, A. Maksimenko, D. T. Bui, J. Mougin and P. Couvreur, *Angew. Chem. Int. Ed.*, 2013, **52**, 1678-1682.
32. T. G. Burke, A. E. Staubus and A. K. Mishra, *J. Am. Chem. Soc.*, 1992, **114**, 8318-8319.
33. E. K. Rowinsky, J. Rizzo, L. Ochoa, C. H. Takimoto, B. Forouzesh, G. Schwartz, L. A. Hammond, A. Patnaik, J. Kwiatek, A. Goetz, L. Denis, J. McGuire and A. W. Tolcher, *J. Clin. Oncol.*, 2003, **21**, 148-157.
34. Y. Y. Pei, M. H. Hong, S. J. Zhu, Y. Y. Jiang, G. T. Tang, C. Sun, C. Fang and B. Shi, *J. Control. Release*, 2010, **141**, 22-29.
35. S. Q. Gao, Z. R. Lu, P. Kopeckova and J. Kopecek, *J. Control. Release*, 2007, **117**, 179-185.
36. M. E. Davis, J. Cheng and K. T. Khin, *Mol. Pharm.*, 2004, **1**, 183-193.
37. J. R. Infante, V. L. Keedy, S. F. Jones, W. C. Zamboni, E. Chan, J. C. Bendell, W. Lee, H. Wu, S. Ikeda, H. Kodaira, M. L. Rothenberg and H. A. Burris, *Cancer Chemoth. Pharm.*, 2012, **70**, 699-705.
38. Y. Shen, E. Jin, B. Zhang, C. J. Murphy, M. Sui, J. Zhao, J. Wang, J. Tang, M. Fan, E. Van Kirk and W. J. Murdoch, *J. Am. Chem. Soc.*, 2010, **132**, 4259-4265.
39. M. E. Fox, S. Guillaudeu, J. M. J. Frechet, K. Jerger, N. Macaraeg and F. C. Szoka, *Mol. Pharm.*, 2009, **6**, 1562-1572.
40. X. Ma, Q. Sun, Z. Zhou, E. Jin, J. Tang, E. Van Kirk, W. J. Murdoch and Y. Shen, *Polym. Chem.*, 2013, **4**, 812-819.
41. Y. Zhang, Q. Yin, L. Yin, L. Ma, L. Tang and J. Cheng, *Angew. Chem. Int. Ed.*, 2013, **52**, 6435-6439.
42. N. Patankar and D. Waterhouse, *Cancer Ther.*, 2012, **18**, 90-104.
43. D. P. Jones, J. L. Carlson, P. S. Samiec, P. Sternberg, V. C. Mody, R. L. Reed and L. A. S. Brown, *Clin. Chim. Acta*, 1998, **275**, 175-184.
44. I. K. Oh, H. Mok and T. G. Park, *Bioconjugate Chem.*, 2006, **17**, 721-727.

45. D. S. Poche, M. J. Moore and J. L. Bowles, *Synth. Commun.*, 1999, **29**, 843-854.
46. Y. Shen, Z. Zhou, M. Sui, J. Tang, P. Xu, E. A. Van Kirk, W. J. Murdoch, M. Fan and M. Radosz, *Nanomedicine-Uk*, 2010, **5**, 1205-1217.

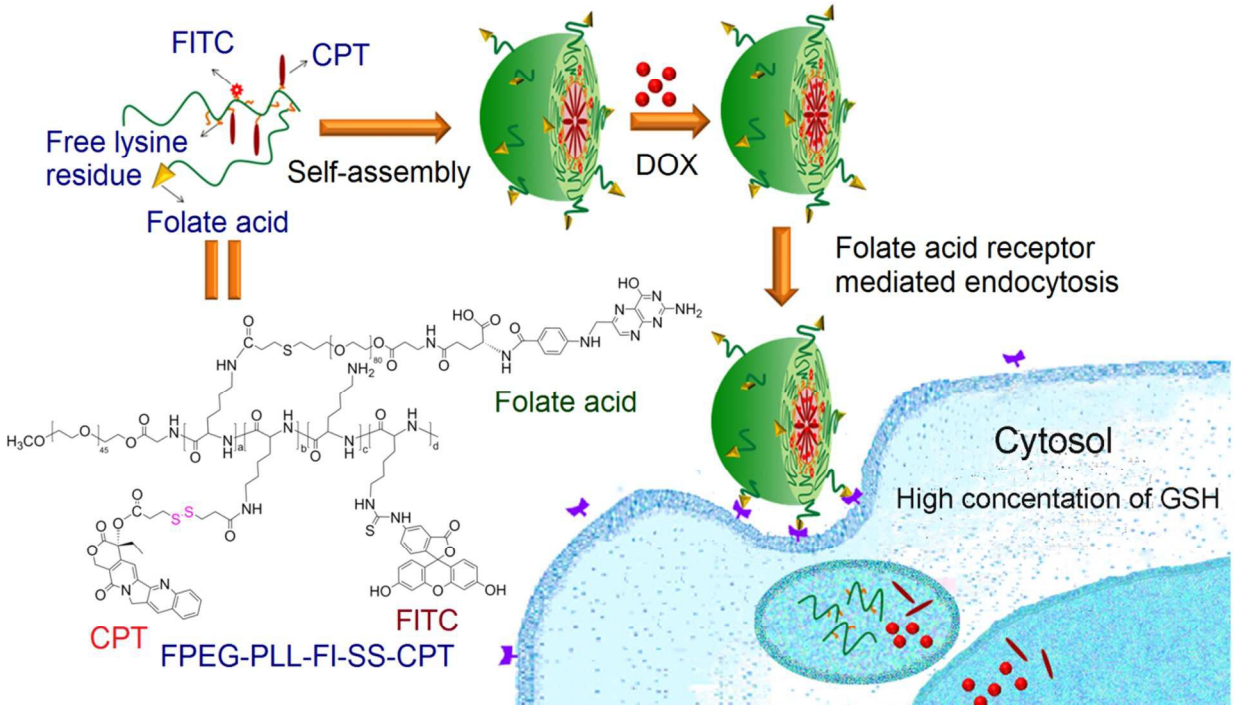

Tumor-targeting CPT-conjugated nanoparticles of high stability and cell-specific drug release were developed for cancer-targeted drug delivery. PEG-PLL was conjugated with a high content of CPT of via a disulfide bond and folic acid via PEG spacer. The conjugate formed CPT-cored nanoparticles with defined drug contents as high as 37.8%, while the micellar size was tailorable by the CPT-content. Such nanoparticles enabled CPT and the loaded drug to be specifically released in cancer cell by GSH-triggered CPT-cleavage and micelle collapse.